chemengineering

MDPI

Article

Synthesis of Non-Cubic Nitride Phases of Va-Group Metals (V, Nb, and Ta) from Metal Powders in Stream of NH_3 Gas under Concentrated Solar Radiation

Nobumitsu Shohoji [1], Fernando Almeida Costa Oliveira [1,*], José Galindo [2], José Rodríguez [2], Inmaculada Cañadas [2], Jorge Cruz Fernandes [3] and Luís Guerra Rosa [3,*]

1 LNEG—Laboratório Nacional de Energia e Geologia I.P., LEN—Laboratório de Energia, UME—Unidade de Materiais para a Energia, Estrada do Paço do Lumiar 22, 1649-038 Lisboa, Portugal; shohoji.nobumitsu@gmail.com

2 CIEMAT—Centro de Investigaciones Energéticas, Medioambientales y Tecnológicas, PSA—Plataforma Solar de Almería, Apartado 22, E-04200 Tabernas, Almería, Spain; jose.galindo@psa.es (J.G.); jose.rodriguez@psa.es (J.R.); i.canadas@psa.es (I.C.)

3 IDMEC—Instituto de Engenharia Mecânica, Instituto Superior Técnico, University of Lisboa, Av. Rovisco Pais, 1049-001 Lisboa, Portugal; cruz.fernandes@tecnico.ulisboa.pt

* Correspondence: fernando.oliveira@lneg.pt (F.A.C.O.); luisguerra@tecnico.ulisboa.pt (L.G.R.)

Abstract: Using a high-flux solar furnace, loosely compacted powders of Va-group transition metal (V, Nb, and Ta) were reacted with stream of NH_3 gas (uncracked NH_3 gas) being heated by concentrated solar beam to a temperature (T) range between 600 and 1000 °C. From V, sub-nitride V_2N (γ phase) and hypo-stoichiometric mono-nitride VN possessing fcc (face-centered cubic) crystal lattice structure (δ phase) were synthesized. On the other hand, in the reaction product from Nb and Ta, hexagonal mono-nitride phase with N/M atom ratio close to 1 (ε phase) was detected. The reaction duration was normalized to be 60 min. In a conventional industrial or laboratory electric furnace, the synthesis of mono-nitride phase with high degree of crystallinity that yield sharp XRD peaks for Va-group metal might take a quite long duration even at T exceeding 1000 °C. In contrast, mono–nitride phase MN of Va-group metal was synthesized for a relatively short duration of 60 min at T lower than 1000 °C being co-existed with lower nitride phases.

Keywords: concentrated solar radiation; uncracked NH_3 gas; nitride; vanadium; niobium; tantalum

Citation: Shohoji, N.; Oliveira, F.A.C.; Galindo, J.; Rodríguez, J.; Cañadas, I.; Fernandes, J.C.; Rosa, L.G. Synthesis of Non-Cubic Nitride Phases of Va-Group Metals (V, Nb, and Ta) from Metal Powders in Stream of NH_3 Gas under Concentrated Solar Radiation. *ChemEngineering* **2021**, *5*, 19. https://doi.org/10.3390/chemengineering5020019

Academic Editor: Ilenia Rossetti

Received: 1 March 2021
Accepted: 16 April 2021
Published: 20 April 2021

1. Introduction

Being inspired by research works of Hägg [1] and of Lehrer [2], both published in 1930, Yoshizawa et al. [3] in 1977 and Shohoji et al. [4] in 1990 used flowing NH_3 gas (uncracked ammonia gas) as the nitriding medium in the nitriding process carried out in a conventional laboratory electric furnace.

In 1992, Katsura [5] published thermodynamic model analysis to rationally interpret the extremely high chemical activity a(N) of N in uncracked NH_3 gas whose extent of dissociation α was suppressed from the equilibrium level α_{eq} of dissociation in a closed reaction chamber.

After 2012, Shohoji et al. [6], Oliveira et al. [7,8], and Fernandes et al. [9] started investigating the reaction between d-group transition metal with uncracked NH_3 gas using heat generated by concentrated solar radiation (instead of using conventional electric furnace). In fact, solar-driven high-temperature technologies are serious candidates to displace the use of electricity or natural gas in the future [10]. In these earlier works [6–9], a spherical glass reaction chamber was used to check for the reactivity of uncracked NH_3 gas for an extensive range of compacted pellet specimens placed in the reactor. The use of a compacted powder pellet was a compromising solution to carry out a test for the maximum number of specimen materials without the risk of cross-contamination in a

limited solar beam time (which is normally the case in a solar furnace). However, in such a configuration with a spherical reactor chamber, the effect of increasing extent of dissociation (α) of flowing NH_3 gas along the flow path from the upstream side to the downstream side was not evaluated. To overcome this problem, we developed a linear flow tube reactor and the first results acquired using this novel reactor setup were published in 2019 [11]. The experiment reported in [11] was done aiming at synthesizing higher nitrides, δ-MoN and ε-Fe_2N, respectively, of Mo and Fe in a stream of NH_3 gas with linear flow speed (v) between 1.14 and 11.4 mm·s^{-1} under heating with concentrated solar beam using the solar furnace SF40 [12] at *Plataforma Solar de Almería* (PSA), Spain, at the processing temperatures T = 800 and 900 °C for tap-densified (loosely compacted) powders of Mo specimen and T = 500 and 600 °C for tap-densified powders of Fe. Specimen powders were placed in four drilled holes of 8 mm in diameter and a depth of 5 mm for rectangular specimen holder block made of refractory steel (ferritic steel with dimensions: length 67 mm, height 20 mm and width 30 mm). The four holes were held at equal distance being designated with P1, P2, P3, and P4 on going from upstream side to downstream side. The distance between the center of P1 and P4 was set to be 45 mm (see Figure 2 in [11]). The volume fraction of higher nitride was greater at P1 than at P4 in respective reaction condition corresponding to increasing extent α of NH3 gas dissociation along the NH_3 flow direction, i.e., decreasing a(N) of uncracked NH_3 gas along the NH_3 flow direction.

In this work, similar experiments were carried out for Va-group transition metals, V, Nb, and Ta, at v = 1.14 and 2.29 mm·s^{-1} for T = 600, 800, and 1000 °C. For the V specimen, hexagonal V_2N phase and fcc VN phase were detected in the reaction products. On the other hand, for M = Nb and Ta specimens, fcc MN phase was not detected but hexagonal MN phase and hexagonal M_2N phase were detected.

Along this text, the empirical phase designation for the M-N system proposed by Brauer and Esselborn [13] is accepted in the following description:

- ε-MN: hexagonal MN;
- δ-MN: fcc MN;
- γ-M_4N_3: tetragonal MN with deficient N at around N/M = 0.75;
- β-M_2N: hexagonal sub-nitride phase;
- α-M(N): primary solid solution of N in metallic M.

As stated by Terao [14], a dissociation of NbN would proceed in the order of ε-NbN $\rightarrow$ δ-NbN $\rightarrow$ γ-Nb_4N_3 according to descending a(N) in the gas environment.

The existence of a γ-M_4N_3 phase was reported for M = Nb but not for M = V and Ta. It is quite likely that Nb_4N_3 corresponds to hypo-stoichiometric NbN whose fcc lattice is subjected to tetragonal distortion on account of the loss of N atoms in the interstitial site with certain regularity. Similar lattice distortion was identified for hypo-stoichiometric zirconium dihydride at around H/Zr ratio 1.72 through an analysis of the equilibrium pressure–temperature–composition (PTC) relationship [15].

Data acquired for nitride synthesis for V, Nb, and Ta in a stream of NH_3 gas under irradiation of a concentrated solar beam are summarized in this report.

2. Experimental

Metal powders of V, Nb, and Ta were subjected to nitridation reactions in the solar furnace SF40, with the nominal power of 40 kW, at PSA [12] in flowing NH_3 gas (Figure 1). Details of the experimental procedures are identical to those described in the paper [11] published in 2019; the only difference are the tap-densified powders (instead of Mo and Fe powders [11], powders of V, Nb, and Ta were subjected to nitridation reactions). At the focal spot of the concentrated solar beam, the radiative flux reaches 7000 Suns (1 Sun = 1 kW·m^{-2}). The amount of the radiative flux was controlled by the angular motion of the louvered shutter blades of the SF40 solar furnace. Heat flux measurements were carried out using a Gardon type radiometer ThermoGage TG1000-1 (Vatell Corporation, Christiansburg, Virginia, U.S.A.), with 0–6469 kW·m^{-2} range. Typically, at 1000 °C radiometer results were in the range of 320 kW·m^{-2}, whereas at 600 °C the values obtained were of

the order of 115 kW·m^{-2}. Moreover, a tilt mirror at 45° was used to perform these tests in a horizontal plane, which turned the focal beam to 90°and projected the concentrated solar beam onto the specimen holder. Extensive range of homogeneity temperature was realized within 10 cm along the NH_3 gas flow path thanks to the temperature homogeniser working by diffusing the concentrated solar beam with multiple-reflection developed at PSA and tested for the first time (Figure 1b). This was essential to enable the influence of decreasing a(N) of uncracked NH_3 along the flow path at a specified temperature over about 5 cm length to be depicted. The homogeniser consists of eight flat mirrors placed in such a way in order to obtain an approximate circular radiation beam incident over the tubular reactor containing the sample holder. Temperature difference among the 8 K-type thermocouples (TC Ltd., Uxbridge, U.K.) fell in the range of ±10 °C (at 600 °C); ±20 °C (at 800 °C) and ±25 °C (at 1000 °C) throughout the test runs performed for 60 min at each set temperature. (Further information about the optical behavior of homogenisers used in high-flux solar furnaces can be found in [16]).

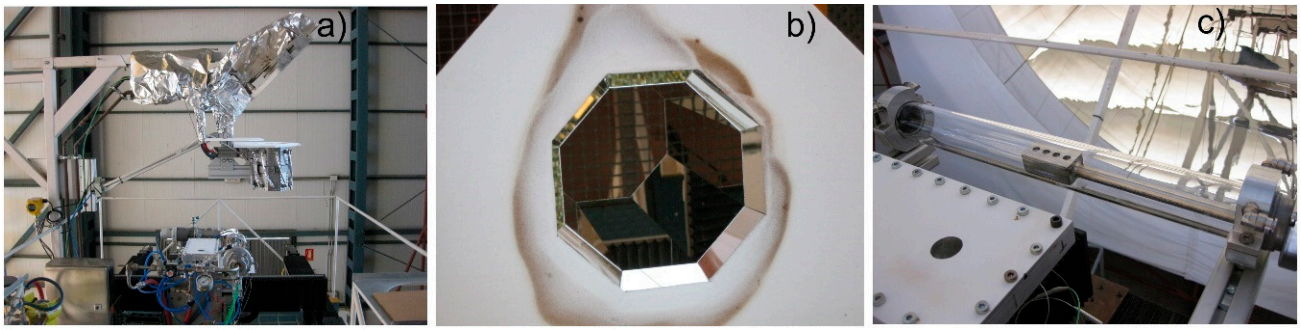

Figure 1. Experimental setup: general view (**a**), top view of the octagonal temperature homogeniser (**b**), and reactor tube containing sample holder (**c**).

Specifications of the reagents used in the present work are listed in Table 1.

Table 1. Specifications of reagents used.

Reagent	Purity [%]	Particle Size [μm]	Supplier
V (powder)	99.0	<45	Goodfellow Cambridge Ltd., Huntingdon, UK
Nb (powder)	99.5	<125	L. Light & Co., Ltd., Colnbrook, UK
Ta (powder)	99.9	<75	Goodfellow Cambridge Ltd., Huntingdon, UK
NH_3 (gas)	99.8	-	Carburos Metálicos, Barcelona, Spain
N_2 (gas)	99.99	-	Carburos Metálicos, Barcelona, Spain

The reactor consisted of a standard 2.5 mm thick borosilicate glass tube with inner diameter of 45 mm and a length of about 1000 mm (Figure 1c). Both ends of the tube were sealed with water-jacketed vacuum flanges to guaranty gas-tightness to avoid undesirable NH_3 leaks and O_2 impurity penetration from the external atmospheric environment. For this purpose, a reactor cooling system has been designed, constructed, and successfully tested at PSA. The reactor was coupled to a gas system allowing both vacuum (10^{-1} mbar) and use of different gases (i.e., NH_3 and N_2) so that an undesirable oxidation of the samples does not occur. The sample holder made of refractory steel contained four holes of 6 mm in diameter and a depth of 3 mm along the NH_3 gas flow path at a 10-mm interval to collect powder samples at different locations along the NH_3 gas stream. The temperature distribution across the powders being tested was monitored by eight K-type thermocouples inserted at the powder top surface and underneath of each sample holding hole; not in direct contact with the NH_3 gas stream. Detailed information on the sample holder and

thermocouples position are provided in Figure 2 in [11]. In addition, an infrared camera and a pyrometer were used to measure the surface temperature on the top surface.

With reference to the experimental conditions used in the aforementioned work [11] carried out for Mo and Fe, two NH_3 flow rate levels, 5 $L \cdot h^{-1}$ (1.14 $mm \cdot s^{-1}$ in linear tubular reactor) and 10 $L \cdot h^{-1}$ (2.29 $mm \cdot s^{-1}$), were tested and three T levels, 600, 800, and 1000 °C were tested. At the gas outlet side of the reactor, dilute HCl aqueous solution was set as a bubbler of the exhaust gas. This was aimed at absorbing residual NH_3 gas contained in the exhaust gas not to dissipate into surrounding environment. When the gas absorption process from NH_3 gas dissociated according to the reaction

$$NH_3 \rightleftarrows (1/2)\, N_2 + (3/2)\, H_2 \quad (1)$$

is in progress, bubbling is anticipated to become less noticeable. Thus, by inspection of mode of the bubbling, the state of the gas absorption process can be estimated. Thence, for constant inspection of the gas bubbling mode during the test run, a video camera to inspect constantly the bubbler surface was installed. By inspecting the bubbler surface, it was proved that H absorption from uncracked NH_3 gas took place at T = 200 °C, as speculated empirically.

After setting the powders to the refractory steel sample holder, the reactor was evacuated to 0.18 mbar by a rotary vacuum pump at ambient temperature and then filled with pure nitrogen (N_2) gas for flushing. This operation was repeated three times before introducing flowing ammonia (NH_3) gas to the reaction chamber at ambient temperature. Powders were then heated under flow of NH_3 gas to a specified reaction temperature (see Table 2).

Table 2. Test conditions and phases identified by XRD.

Test Run	Sample	Temperature [°C]	Phases Identified
T1–1	Nb	800	Nb, NbO, Nb_2N
T1–4	Nb	800	Nb, NbO, Nb_2N
T2–1	V	800	V_2N, VN
T2–4	V	800	V_2N, VN
T3–1	Ta	800	Ta_2N, Ta
T3–4	Ta	800	Ta_2N, Ta
T7–1	Nb	600	Nb
T7–4	Nb	600	Nb
T8–1	V	600	$V_{16}N_{1.5}$, V_2N
T8–4	V	600	$V_{16}N_{1.5}$
T9–1	Ta	600	Ta, $TaN_{0.1}$
T9–4	Ta	600	Ta
T13–1	Nb	1000	Nb_2N, NbN
T13–4	Nb	1000	Nb_2N, NbN
T14–1	V	1000	VN
T14–4	V	1000	VN (traces V, V_2N)
T15–1	Ta	1000	TaN, Ta_2N, Ta
T15–4	Ta	1000	TaN, Ta_2N, Ta

Once the reaction duration at temperature has reached completion, gas was changed from NH_3 to N_2 (flowing at 5 $L \cdot h^{-1}$ maintaining the temperature at T for 5 min). This was to ensure full substitution of the reaction chamber environment to N_2 gas from NH_3 before starting to cool down. This precaution to substitute gas from NH_3 to N_2 at the onset of cooling immediately after the end of the nitriding reaction was taken to minimize loss of N from the nitrided specimen surface during cooling.

Table 2 lists the test conditions carried out at the PSA SF40 solar furnace for Nb, V, and Ta powder specimens in stream of NH_3 gas (uncracked NH_3) under irradiation of concentration solar beam at fixed duration (60 min) and NH_3 flow rate (1.14 $mm \cdot s^{-1}$). T1–1 refers to test run 1 and sample at position 1 (closest to the gas stream inlet) whereas T1–4

denotes the same test run but sample at position 4 (i.e., closest to the gas stream outlet), and so on. Phase identification data are given in the following section.

X-ray diffraction (XRD) analysis was performed using a Panalytical XPert Pro MPD diffractometer in the Bragg–Brentano configuration. The data were collected with a step size of 0.02° using an X'Celerator 1D detector using CuKα1 radiation with the wavelength of 1.5406 Å, having the accelerating voltage of 40 kV.

3. Results and Discussion

3.1. Nitriding under Flowing NH_3

Temperature profiles were consistently recorded throughout experiments carried out in each day for individual test runs. Typical temperatures profiles gathered for the nitridation reactions of V, Nb, and Ta with NH_3 stream at both 800 °C and 1000 °C are given in Figure 2.

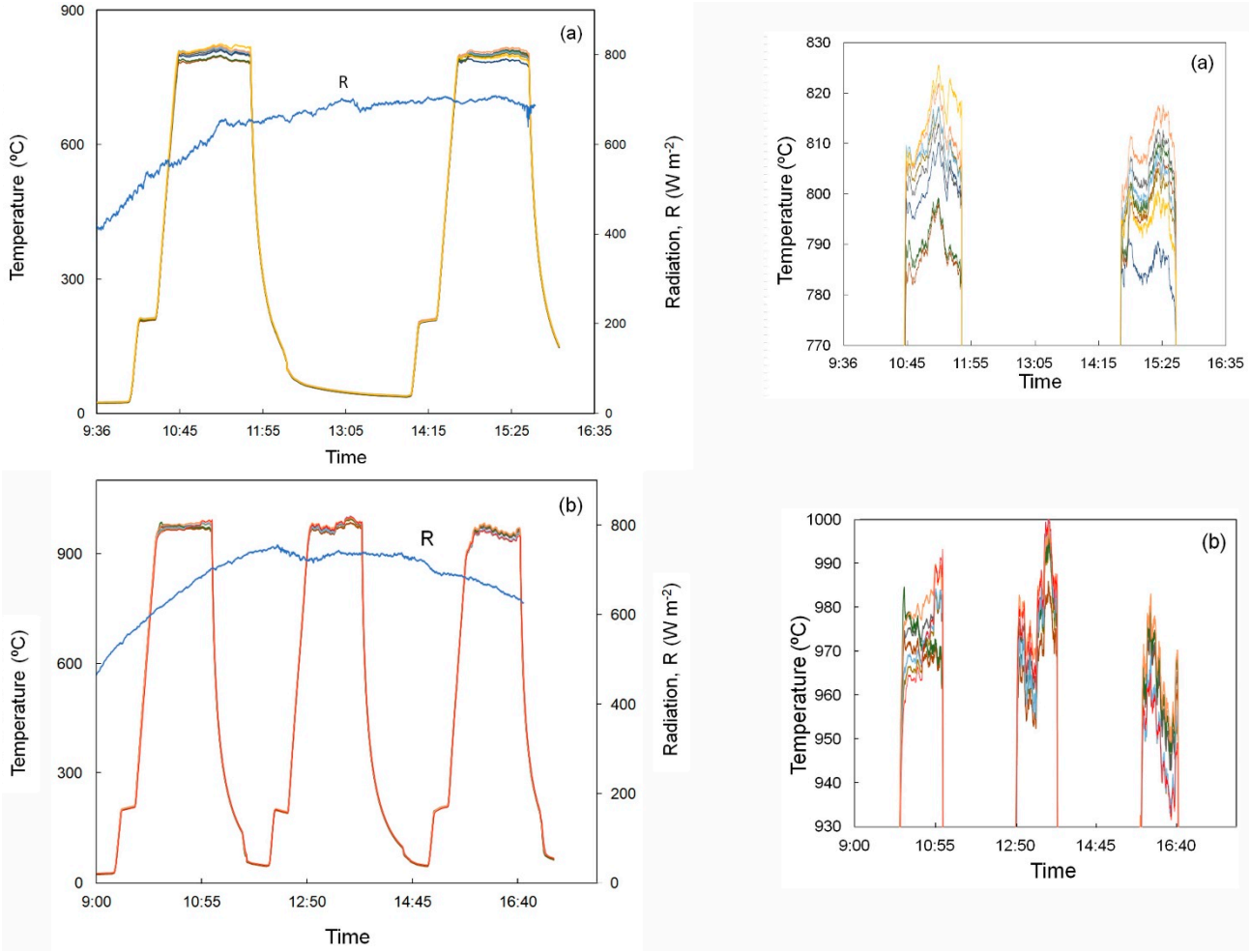

Figure 2. Temperature profiles recorded at 800 °C (**a**) and 1000 °C (**b**) showing data measured by the 8 K-type thermocouples placed at different heights (cf. Figure 2 in [11] and inserts) together with the solar radiation flux density measured throughout each test run.

The most striking features of Figure 2 are (i) the homogenous temperature distribution across the height of the samples and (ii) the close relationship between the radiation and the temperature control, which is particularly visible during the dwell times at the set temperatures. This is related to the presence of mist or clouds that decrease the otherwise expected direct normal irradiance (DNI) normally around 1000 $W \cdot m^{-2}$ under clean sky conditions. The eight thermocouple readings are pretty superimposed indicating that the use of the homogeniser and the refractory steel holder were very effective in guaranteeing

a steady flux of radiation, and consequently a very stable temperature along the 60 min plateau. This suggests that the current setup is suitable to carry out materials testing under well controlled temperatures and flow rates in the absence of O_2 impurities. Moreover, the metal powder specimens distributed among the holes drilled on the sample holder allowed the effect of the gas stream along the flow of the reaction gas to be evaluated. This provided additional information on the influence of nitrogen activity along the flow path as NH_3 is consumed by the reaction with the metal powders as it flows from the inlet to the outlet of the reactor tube.

Looking at the time-variation pattern of bubbling set at the gas exhaustion end of the reactor system, hydridation reduction of oxide scale with hydrogen that comes from dissociated ammonia was ensured to take place at 15 min T–holding duration and 200 °C and, up to 600 °C, such reaction was surely commenced (Figure 3), being dependent on the material (e.g., in case of V the hydridation took place at temperatures as low as 135 °C). During the first test run, the table moved upwards and the reactor collided with it and broke down, owing to a water leakage in the homogeniser cooling circuit. It was necessary to replace the borosilicate glass tube with a new one. In this case, a blank test was then carried out at 200 °C for 15 min in order to remove the oxide layer resulting from the contact of water with the Nb powder. This procedure was not sufficient to fully eliminate the oxide formed, as traces of NbO were still present in the Nb samples exposed at 800 °C for 60 min under flowing NH_3 (1.14 mm·s^{-1}).

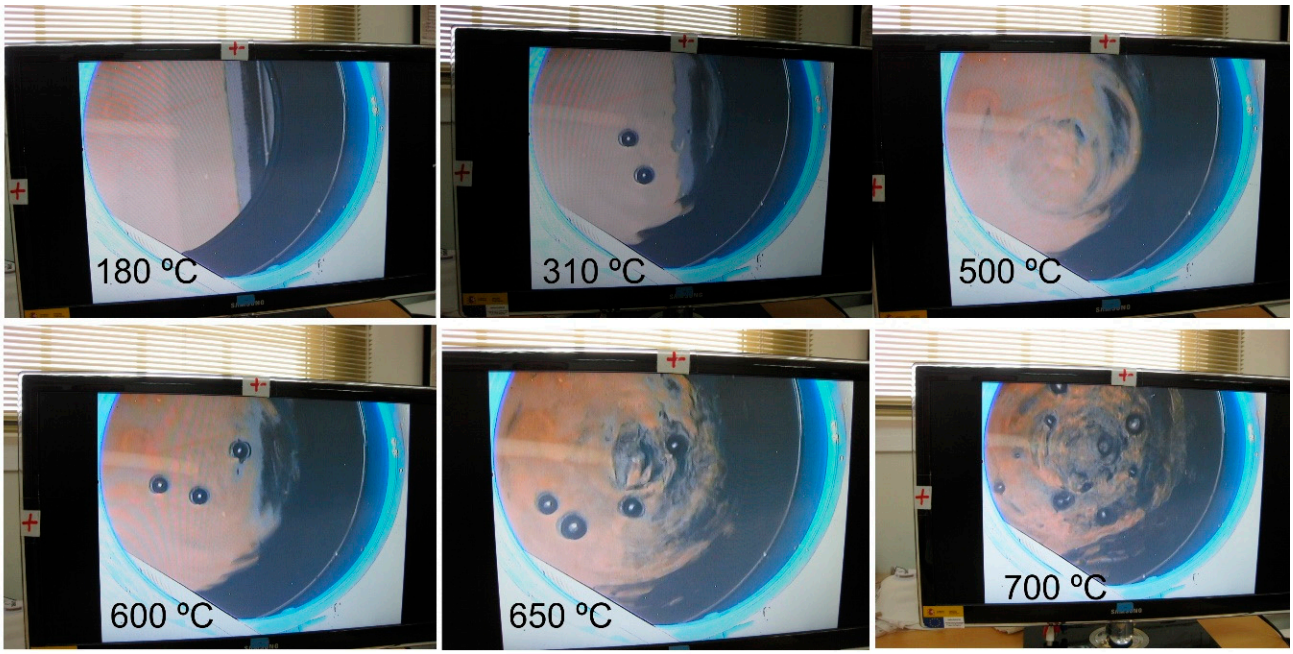

Figure 3. Typical example of bubbles evolution as a function of T during nitriding of Ta powder at 800 °C, for 60 min, and 10 L·h^{-1} NH_3.

In the case of V powder, bubble formation was not observed around 135 °C, suggesting that the gas was consumed. Above 670 °C, bubbles were again observed and the rate of formation increased with increasing the temperature. A similar pattern was observed for Nb powder. As for Ta powder, only at around 180 °C bubbles stopped forming. Between 300 and 400 °C, sporadically one bubble was observed. Above 500 °C, the bubbling process was no longer visible, and bubbles were seen again around 610 °C. With increasing temperature, the bubble rate formation increased slowly and at around 700 °C, the regime was similar to that observed for the V and Nb.

3.2. X-ray Diffraction Analysis

N/M ratio x in the synthesized MN_x varied depending on a(N) of uncracked NH_3 that is determined depending on the extent of dissociation α of NH_3 that increases along the flow line of NH_3 gas on going from up-stream to down-stream side at given T (600, 800, and 1000 °C) and NH_3 gas flow rate (5 and 10 $L \cdot h^{-1}$ or, in terms of linear flow rate, 1.14–2.29 $mm \cdot s^{-1}$) in the used tubular reactor setup. Only the most advantageous conditions for nitriding were evaluated by XRD analysis, i.e., lowest flow rate and position 1 (nearest to gas inlet in the reactor), except in the case of Ta powders.

3.2.1. Vanadium

The X-ray diffraction (XRD) profiles of chemically prepared V nitride powders, in the range of $30° < 2\theta < 140°$ with a step size of 0.02°, are shown in Figure 4. The diffraction pattern shows peaks corresponding to the planes, which matches with the pattern of the Joint Committee on Powder Diffraction Standards (JCPDS), having the card no. 071-1230 (corresponding to the phase $V_{16}N_{1.5}$/●/) and traces of V_2N/□/(ICDD card no. 033–1439) at a temperature as low as 600 °C. With increasing temperature, from 600 to 800 °C, it becomes evident that the main phase V_2N (ICDD card no. 071-0618) is present and traces of VN (ICDD card no. 008-3866) become discernible. At 1000 °C, only the VN phase/♦/(ICDD card no. 035-0768) is evident. This evidence clearly indicates that the extent of nitridation of V powders is temperature dependent and it follows the expected trend. After exposure to 600 °C, no evidence of V_2N could be depicted in the sample in P4. The reasoning will be provided below when the data for Ta shall be discussed.

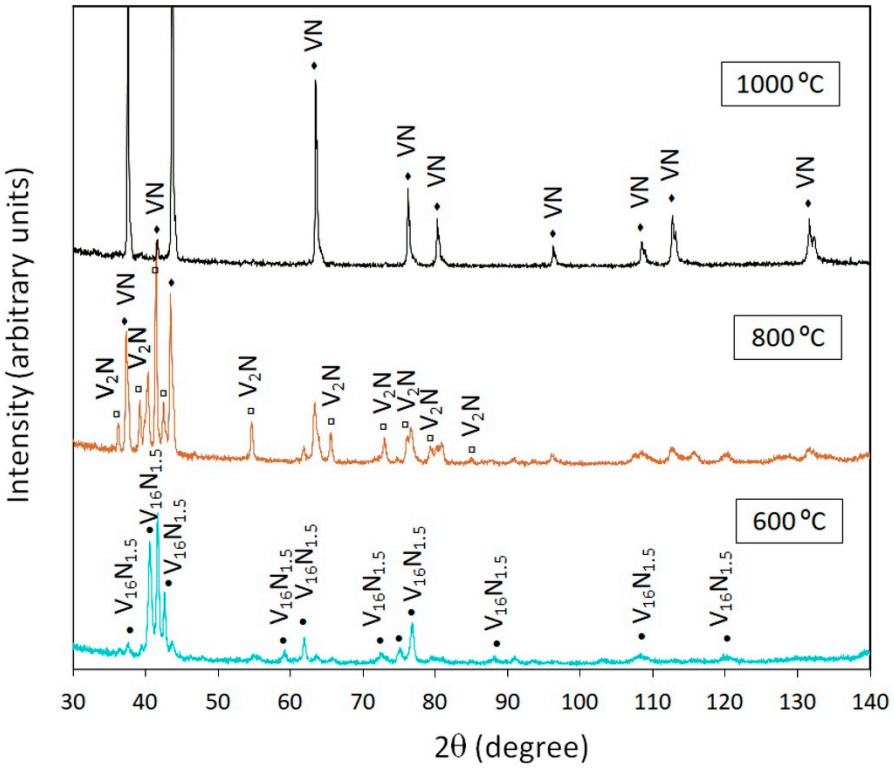

Figure 4. XRD patterns obtained for V powders nitrided under flowing NH_3 (1.14 $mm \cdot s^{-1}$).

3.2.2. Niobium

Data for Nb powders nitrided under the same nitriding conditions, in the range of $30° < 2\theta < 80°$ with a step size of 0.02°, are shown in Figure 5. Unlike in the case of V, no nitrides were formed at a temperature as low as 600 °C. In fact, only peaks corresponding to the phase Nb/●/(ICDD card no. 005-1416) were identified. When the temperature was increased to 800 °C, in addition to V, the formation β-Nb_2N/□/(ICDD card no. 040-1274)

took place; peaks non-identified correspond to NbO traces (ICDD card no. 074-1709). The presence of the oxide phase suggests that the preliminary treatment performed prior to testing at 800 °C was not efficient enough in removing oxides formed owing to the reactor break incident. Although complete nitridation of Nb could not be accomplished at 1000 °C, under the conditions used, NbN/♦/(ICDD card no. 020-0801) mixed with Nb_2N (ICDD card no. 075-0952) were formed, indicating that the single NbN could not be synthesized, as in the case of V powders. These results are consistent with available data [13–15,17,18]. There exist six phases, viz. α, β, γ, δ, δ′, and ε, depending upon the thermal conditions and gases (either N_2 or NH_3) used [13]. Typically, nitride phases were only formed above 750 °C.

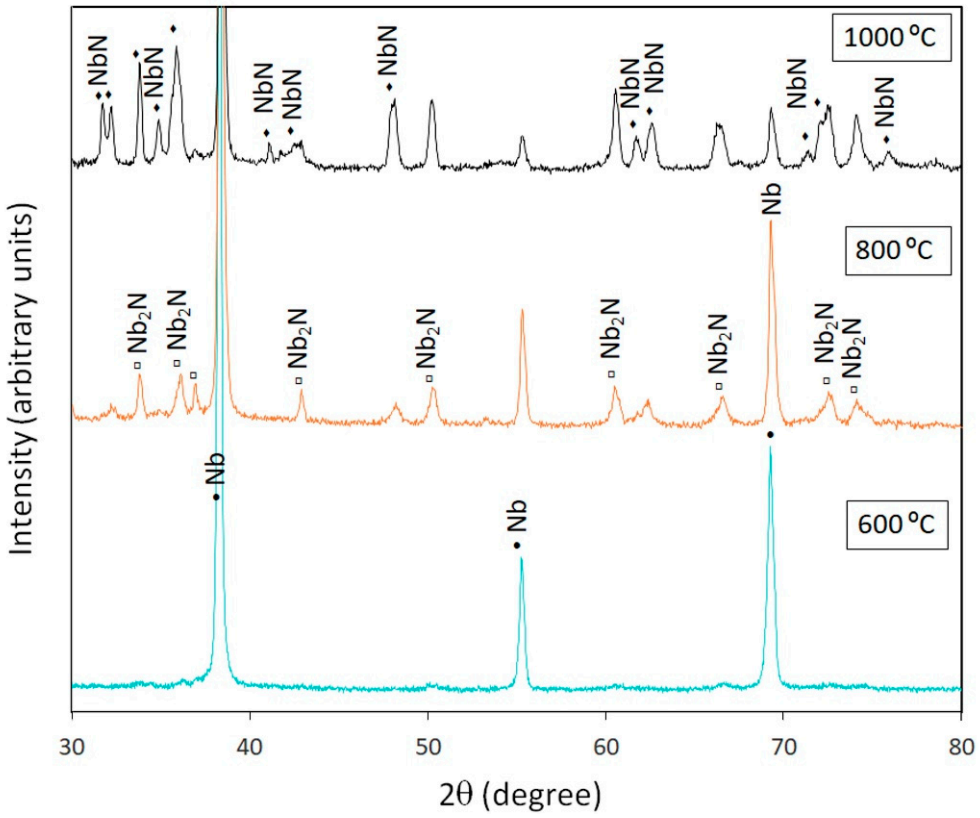

Figure 5. XRD patterns obtained for Nb powders nitrided under flowing NH_3 (1.14 $mm \cdot s^{-1}$).

Unlike in the case of nitriding under flowing NH_3 gas, nitridation of cubic δ-NbN in molecular N_2 atmosphere requires either high temperatures (1300–1450 °C) [17] and/or high pressures (e.g., 4 MPa) [18]. This is related to the fact that nitridation conducted in ammonia-flow clearly exhibited the higher reactivity of NH_3 in comparison with molecular nitrogen.

3.2.3. Tantalum

A similar trend detected for Nb was also observed for Ta powder (Figure 6). In fact, no nitride phases were formed at 600 °C in amounts detectable by XRD. The only phase present matches the ICDD card no. 001-1182 of Ta. At 800 °C, it is possible that both tantalum sub-nitrides were formed as peaks seem to correspond to a mix of β-Ta_2N (ICDD cards no. 026-0985 and no. 029-1321, respectively). This is not surprising since β-Ta_2N and δ-TaN have broad composition ranges and are typical nonstoichiometric compounds. Only when the nitriding temperature reaches 1000 °C, the formation of ε-TaN (fcc) is observed together with β-Ta_2N. δ-TaN has the NaCI structure [19], and β-Ta_2N a structure similar to that of β-Nb_2N [20]. An exothermic reaction between tantalum and nitrogen has been reported at around 800 °C. For comparison purposes, the XRD patterns obtained for

samples from P1 (position 1: the nearest to gas inlet) and P4 (position 4: the closest to gas outlet) are also shown in Figure 6 for both 800 and 1000 °C. Only slight differences in peak intensity can be observed. Typically, the peaks are sharper and more intense for samples in P1 when compared to ones in P4. In fact, high nitrogen activity may arise from the suppressed extent of dissociation α of NH_3 stream and ought to increase with increasing temperature at any given extent of dissociation, which in turn depends on flow rate [5]. Therefore, the use of a stream of NH_3 makes it possible to prepare nitrogen-rich metal nitride, which cannot be obtained when using molecular N_2 even at elevated pressure of few hundred atmospheres. On the other hand, the extent of ammonia dissociation was also found to vary across the various positions along the flow of the reaction gas [21] and with particle size [22]. In case of iron, nanoparticles were found to enhance ammonia dissociation and the product was therefore of lower nitrogen content than that of coarse particles [22].

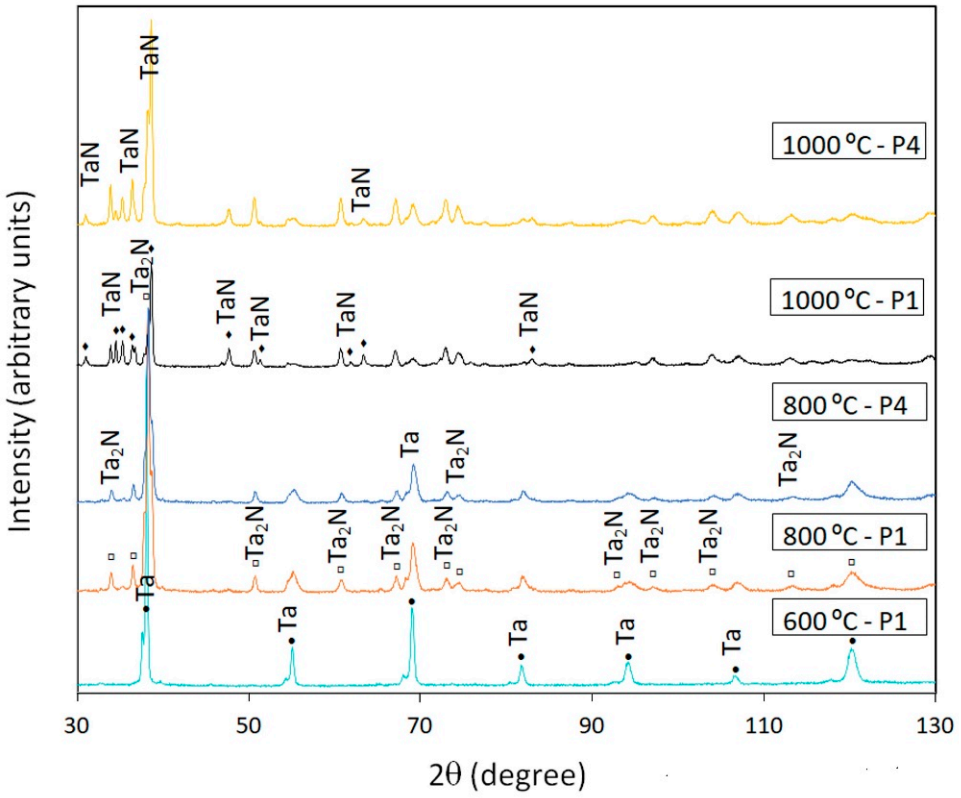

Figure 6. XRD patterns obtained for Ta powders nitrided under flowing NH_3 (1.14 mm·s^{-1}) where P1 refers to position 1 nearest to gas inlet and P4 refers to position 4 closest to gas outlet.

A structure for β-Ta_2N has been proposed with tantalum atoms in a hexagonal close packing (hcp) lattice and the nitrogen atoms randomly distributed in the octahedral holes of the hcp lattice [23]. A comprehensive review of the phases that can form when powdered Ta reacts with ammonia in the temperature range between 700 and 1100 °C for times varying between 1 h and 2 weeks was presented by Schönberg [24]. He found that homogenous stoichiometric ε-TaN was formed at 1000 °C over three days, but no mention was made to the gas flow rate used (merely that "a constant and relatively fast stream of the gas (ammonia) was passed through a silica tube furnace"). It is not therefore surprising that it was not possible to obtain such compound alone only after 1 h of exposure to the solar beam. The peaks recorded match those of the ICDD card no. 008-9907. The reaction involves both dissolution of nitrogen in the tantalum metal and nitride formation. Nitrogen dissolution predominates during the initial stages of the reaction. Below 1000 °C mainly Ta_2N is formed, while above this temperature $TaN_{0.8–0.9}$ and TaN are the main reaction products. The ε-TaN was typically prepared by annealing tantalum nitride in nitrogen at

1450 °C and 1.4 MPa for 70 h and its structure, first determined by XRD patterns [23], was later confirmed by neutron diffraction data [25].

Tantalum nitrides exist in various stable and metastable phases (more than 11), such as TaN, Ta_3N_5, Ta_4N_5, and Ta_5N_6, with various applications, including coatings, photocatalysis, and supercapacitors [26]. Semiconductive nitrogen-rich tantalum nitrides, including Ta_4N_5 and Ta_3N_5, were successfully synthesized via an ammonia looping process through thermal decomposition of Ta-$(NCNH_2)_x$ precursor. Such approach considerably reduces ammonia usage in comparison to conventional nitridation methods.

Another area of application of transition metal nitrides (TMNs) deals with advanced catalysts for electrochemical water splitting [27]. Although considerable development has been achieved, there is plenty of room for improvement of the catalytic properties of TMNs in hydrogen and oxygen evolution reactions together with the need to design efficient non-noble metal-based catalysts.

4. Conclusions

Va-group transition metal (V, Nb, and Ta) powders were successfully nitrided under well controlled flowing NH_3 gas for the first time using direct concentrated solar beam radiation in a solar furnace at temperatures above 800 °C.

Successful nitriding of V was accomplished just after 1 h of exposure to solar radiation at 1000 °C for the first time. This is related to the tight control of temperature and oxygen impurities achieved with the new designed experimental setup used.

Mixed nitrides of Nb and Ta were obtained, thereby suggesting that further work is needed to understand whether increase of exposure time would eventually result in the formation of single-phase stoichiometric MN, as in the case of V, or not. Raising temperatures results in undesired decomposition of NH_3 and consequent decrease of nitrogen activity, so temperature ought to be as low as possible.

Nitrides of Va-group transition metals are gaining considerable interest in various promising applications. Indeed, vanadium nitride (VN) was proposed as an active catalyst for the electrochemical nitrogen reduction reaction to ammonia as a negative electrode material for supercapacitors for energy storage. In turn, niobium nitride (NbN), in the form of thin films, are the best choice for fabricating efficient superconducting single-photon detectors for the visible and near infrared spectrum. On the other hand, tantalum nitride (TaN) thin films are, in particular, attractive for use as resistors and diffusion barriers in semiconductor technology. The nitride powders obtained in the present work can be regarded as precursors for making new devices using thin film sputtering techniques.

Author Contributions: N.S. and F.A.C.O.: conceptualization, methodology, data curation, validation, writing—original draft preparation. J.G., J.R., and I.C.: solar experimental resources. J.C.F.: methodology, experimental resources, sample preparation. L.G.R.: formal analysis, writing—review and editing, project administration. All authors have read and agreed to the published version of the manuscript.

Funding: The authors were beneficiaries of the Solar Facilities for the European Research Area (SFERA) Programme (SFERA-III Project Grant Agreement no. 823802) which allowed them to carry out a test campaign at the CIEMAT-PSA solar furnace SF40. This research was partially funded by the Portuguese Foundation for Science and Technology (FCT), through IDMEC, under LAETA, project UIDB/50022/2020. The funding provided by FCT to INIESC—National Research Infrastructure for Concentrated Solar Energy through contract ALT20-03-0145-FEDER-022113 is also thanked.

Acknowledgments: The technical assistance of Fabian Sola (PSA), Isabel Figueira (LNEG), Joana Pinto (FCT/UNL), and the administrative support of Marta Ruiz are greatly appreciated.

Conflicts of Interest: The authors declare no conflict of interest.

References

1. Hägg, G. X-radiation experiments on molybdenum nitrides and tungsten nitrides. *Z. für Phys. Chem. -Abt. B* **1930**, *7*, 339–362.
2. Lehrer, E. Iron-hydrogen-ammoniac balance. *Z. für Elektrochem. und Angew. Phys. Chem.* **1930**, *36*, 383–392.
3. Yoshizawa, H.; Shohoji, N.; Katsura, M.; Sano, T.; Yato, T. Nitrierung des metalls bzw. metallcarbides unter ammoniakstrom. *Technol. Rep. Osaka Univ.* **1977**, *27*, 363–370.
4. Shohoji, N.; Marcelo, T.; Katsura, M. Influence of metastable species (non-graphitic carbon and ammonia gas) in the reactants on the composition of the reaction product (carbide, carbo-nitride and nitride). *Solid State Ion.* **1990**, *38*, 187–194. [CrossRef]
5. Katsura, M. Thermodynamics of nitride and hydride formation by the reaction of metals with flowing NH_3. *J. Alloys Compd.* **1992**, *182*, 91–102. [CrossRef]
6. Shohoji, N.; Oliveira, F.A.C.; Fernandes, J.C.; Rosa, L.G.; Rodríguez, J.; Cañadas, I.; Ramos, C.; Magalhães, T.; Cestari, F. Synthesizing higher nitride of molybdenum (Mo) and iron (Fe) in ammonia (NH_3) gas stream under irradiation of concentrated solar beam in a solar furnace. *Mater. und Werkst.* **2013**, *44*, 959–971. [CrossRef]
7. Oliveira, F.A.C.; Rosa, L.G.; Fernandes, J.C.; Rodríguez, J.; Cañadas, I.; Magalhães, T.; Shohoji, N. Nitriding VIa-group metals (Cr, Mo and W) in stream of NH_3 gas under concentrated solar irradiation in a solar furnace at PSA (Plataforma Solar de Almería). *Sol. Energy* **2015**, *114*, 51–60. [CrossRef]
8. Oliveira, F.A.C.; Vasques, I.F.; Fernandes, J.C.; Cañadas, I.; Rodríguez, J.; Rosa, L.G.; Shohoji, N. Reactions of IVa-group metals, Ti and Zr, with uncracked NH_3 gas at a temperature in the range between 600 and 800 °C under heating with concentrated solar beam at PSA. *Sol. Energy* **2016**, *138*, 119–127. [CrossRef]
9. Fernandes, J.C.; Oliveira, F.A.C.; Rosa, L.G.; Rodríguez, J.; Cañadas, I.; Magalhães, T.; Shohoji, N. Low-temperature short-time nitriding of Va-group metals, V, Nb and Ta, in uncracked NH_3 gas under heating with concentrated solar power (CSP). *Ciência Tecnol. dos Mater.* **2016**, *28*, 112–116. [CrossRef]
10. Rosa, L.G. Solar heat for materials processing: A review on recent achievements and a prospect on future trends. *ChemEngineering* **2019**, *3*, 83. [CrossRef]
11. Shohoji, N.; Oliveira, F.A.C.; Galindo, J.; Fernandes, J.C.; Rodríguez, J.; Cañadas, I.; Rosa, L.G. Influence of linear flow velocity of uncracked ammonia (NH_3) gas on formation of higher nitrides, δ-MoN and ε-Fe_2N, under concentrated solar irradiation in the SF40 solar furnace at PSA. *Int. J. Mater. Chem.* **2019**, *9*, 1–12. [CrossRef]
12. Rodríguez, J.; Cañadas, I.; Zarza, E. New PSA high concentration solar furnace SF40. *AIP Conf. Proc.* **2016**, *1734*, 070028. [CrossRef]
13. Brauer, G.; Esselborn, R. Nitridphasen des niobs. *Z. für Anorg. und Allg. Chem.* **1961**, *309*, 151–170. [CrossRef]
14. Terao, N. Structure des nitrures de niobium. *Jpn. J. Appl. Phys.* **1965**, *4*, 353–367. [CrossRef]
15. Shohoji, N.; Marcelo, T. Tetragonality in crystal lattice of zirconium dihydride. *J. Mater. Sci. Lett.* **1987**, *6*, 1251–1253. [CrossRef]
16. Pereira, J.C.G.; Rahmani, K.; Rosa, L.G. Computer modelling of the optical behaviour of homogenisers in high-flux solar furnaces. *Energies* **2021**, *14*, 1828. [CrossRef]
17. Brauer, G.; Jander, J. Die nitride des niobs. *Z. für Anorg. und Allg. Chem.* **1952**, *270*, 160–178. [CrossRef]
18. Lengauer, W.; Ettmayer, P. Preparation and properties of compact cubic δ-NbN_{1-x}. *Mon. für Chem. Chem. Mon.* **1986**, *117*, 275–286. [CrossRef]
19. Gatterer, J.; Dufek, G.; Ettmayer, P.; Kieffer, R. The cubic tantalum mononitride (B1) and its miscibility with the isotypic mononitrides and monocarbides of the 4a and 5a group metals. *Mon. für Chem. Chem. Mon.* **1975**, *106*, 1137–1147. [CrossRef]
20. Conroy, L.E.; Christensen, A.N. Preparation and crystal structure of β-Ta_2N. *J. Solid State Chem.* **1977**, *20*, 205–207. [CrossRef]
21. Nishimaki, K.; Nakagawa, T.; Yamamoto, T.A.; Katsura, M. Equilibrium between flowing NH_3 and synthesized FeN_x at various positions along flow of reaction gas. *Technol. Rep. Osaka Univ.* **1998**, *48*, 153–156.
22. Nishimaki, K.; Ohmae, S.; Yamamoto, T.A.; Katsura, M. Formation of iron–nitrides by the reaction of iron nanoparticles with a stream of ammonia. *Nanostruct. Mater.* **1999**, *12*, 527–530. [CrossRef]
23. Brauer, G.; Zapp, K.H. Die nitride des tantals. *Z. für Anorg. und Allg. Chem.* **1954**, *277*, 129–139. [CrossRef]
24. Schönberg, N. An X-ray study of the tantalum-nitrogen system. *Acta Chem. Scand.* **1954**, *8*, 199–203. [CrossRef]
25. Christensen, A.N.; Lebech, B. A reinvestigation of the structure of ε-tantalum nitride. *Acta Crystallogr.* **1978**, *B34*, 261–263. [CrossRef]
26. Lin, J.; Zhao, W.; Huang, F. Facile and economical synthesis of nitrogen-rich tantalum nitrides via an ammonia looping process under confined space. *New J. Chem.* **2020**, *44*, 9158–9162. [CrossRef]
27. Peng, X.; Pi, C.; Zhang, X.; Li, S.; Huo, K.; Chu, P.K. Recent progress of transition metal nitrides for efficient electrocatalytic water splitting. *Sustain. Energy Fuels* **2019**, *3*, 366–381. [CrossRef]